


Real-Time Monitoring of Displacement of Machine Vision Bridge Based on YOLOV5-MLR Study

Dong Ran^{1,2,*}^a, Jianxu Long^{1,2}^b, Zhuan Wang^{1,2}, Xiaoyong Zhang^{1,2} and Qian Guo^{1,2}

¹Department of Architectural Engineering, Guizhou Communications Polytechnic University, Guiyang 551400, China

²Key Laboratory of High Performance Repair Materials, Guizhou Communications Polytechnic University, Guiyang 551400, China

*

Keywords: Bridge Monitoring, Target Detection, Target Recognition, Displacement Monitoring.

Abstract: Currently, the bridge maintenance tasks are arduous, and the health condition of bridges is of the utmost importance to ensure traffic safety. In order to achieve real-time monitoring of bridges and reduce monitoring costs, it is necessary to seek practical and effective solutions. Research has found that due to the influence of environmental and other factors, the precision and accuracy of traditional machine vision monitoring methods are insufficient. Therefore, this paper proposes a method called the YOLOV5-MLR improved algorithm. This algorithm adopts more complex texture targets and can better distinguish the surrounding environment during the monitoring process, thus improving the accuracy. In addition, during the calculation process, the algorithm refines the precision unit to the pixel level and can achieve a precision level at the sub-millimeter level. After a series of experimental verifications, the results show that the YOLOV5-MLR improved algorithm has high robustness, and the monitoring error is controlled at the millimeter level, meeting the specification requirements for bridge monitoring. This new algorithm provides important technical support for bridge health monitoring and is expected to play a key role in the field of bridge monitoring.


1 INTRODUCTION


Currently, for the monitoring of buildings, slopes and bridges, the main equipment used are total stations and RTK. The total station has relatively high precision and is the mainstream equipment for monitoring. (Liu et al., 2024; Liao et al., 2024; Shan et al., 2024) However, it requires continuous operation by personnel to complete the measurement work at monitoring points. Meanwhile, the cost of total station equipment is relatively high. The positioning accuracy of RTK is around 2 cm, which to some extent has an impact on the monitoring results. In addition, after collecting data through sensors, some scholars conduct manual marking in the way of image annotation. Although this method has relatively high precision, its efficiency is low and it requires post-processing for coordinate staking.

Some scholars also detect the center of the target by means of corner detection (Liu, Y et al., 2024,

Shang et al., 2024; Bao et al., 2024). For example, (Busca et al., 2024) developed a vision-based displacement sensor system by utilizing pattern matching, edge detection and digital image techniques. Two different visual sensors were used to track the high-contrast target fixed on the bridge and measure the vertical displacement of the bridge. Harris corner detection sets a predefined rectangular window, moves it slightly in all directions in the image, and identifies corners according to the gray level changes of the image inside the window (Shang et al., 2024; Xiang et al., 2010). SUSAN corner detection adopts a nearly circular template and sets the center point of the template as the core point (Lin et al., 2010). A pixel point and a sufficient number of different regional pixels around it are defined as FAST corners (Ding et al., 2013).

For uncomplicated targets, this method can quickly and accurately identify the center of the target. However, when affected by the surrounding

^a <https://orcid.org/0009-0004-6775-2992>

^b <https://orcid.org/0000-0003-3067-448X>

environment and the problems of the camera itself, resulting in low-quality collected images or in the case of targets with complex textures, using the corner detection method will simultaneously obtain multiple detection targets, and the accuracy will be interfered to some extent. Moreover, manual processing will still be required in the later stage.

In addition to corner detection, some scholars also use tracking and target detection methods for displacement detection. (Lee et al., 2012) proposed a corner measurement system for large civil structures based on computer vision. By utilizing image processing technology, they tracked artificial targets and calculated the rotation angles. (Hu et al., 2022) used the computer vision-based method to identify the displacements of multiple targets. At present, deep learning methods are mostly adopted for target recognition, such as the YOLO series of algorithms for target detection (Zhou et al., 2023), which can quickly identify the positions of targets and quickly obtain the central coordinates of targets according to the prior boxes. However, due to the influence of factors such as the shooting angle and the target angle, the coordinates of the target center are not accurate. Therefore, based on the YOLOv5 target detection algorithm, this paper adds the MLR (Multiple Linear Regression) method to quickly and accurately determine the central position of the target according to the gray values of the image.

2 DISPLACEMENT MONITORING BASED on the IMPROVED YOLOV5-MLR ALGORITHM

2.1 The Principle of Displacement Measurement in Computer Vision

Two-dimensional coordinate displacement monitoring of the monitored object is carried out through the means of computer vision. The calculation is mainly based on several parameters such as the distance from the camera to the monitored object, the focal length of the camera, the image resolution and the number of displacement pixels, as shown in the following Figure 1:

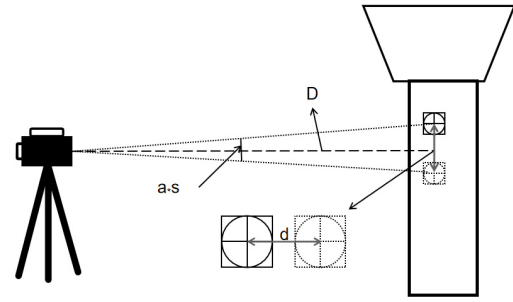


Figure 1: Schematic diagram of the target displacement measurement with computer vision.

Among them, D represents the distance from the camera to the target, a represents the pixel size of the camera, s represents the number of pixels by which the target has changed before and after displacement, and the focal length f is a known value. According to formula (1), the distance of the target before and after displacement can be calculated.

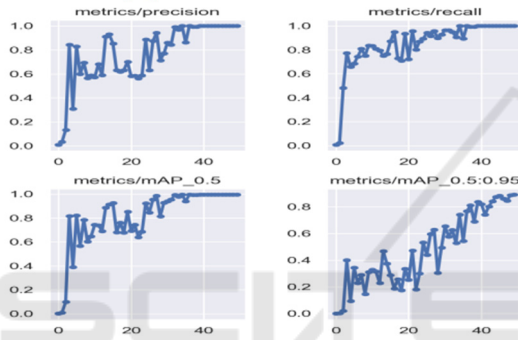
$$d = D * a * s / f \quad (1)$$

During the entire calculation process, d is a variable that requires measurement and calculation. Therefore, only by accurately obtaining the centers of the targets before and after the change can the displacement of the targets be calculated accurately. When the value of d increases, a single pixel also has a relatively large impact on the accuracy of the measurement data. Hence, it is necessary to adopt a high-precision method for obtaining the centers of the targets so as to ensure the accuracy of bridge displacement monitoring.

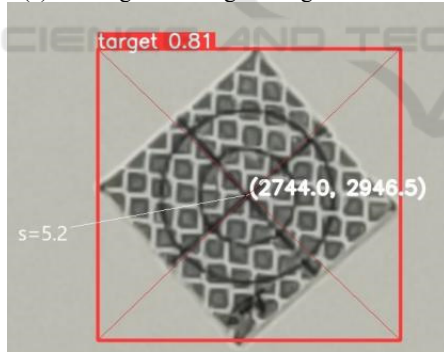
2.2 Extraction of the Initial Coordinates of Feature Points Based on YOLOV5

Affected by factors such as the environment, the angle of the target, the deformation of the target, and the bounding box (BOX), although the YOLOV5 algorithm cannot accurately identify the center point of the target, it can obtain an approximate coordinate. It can quickly calculate the center coordinate of a target through the four corner points of the bounding box. Therefore, the research in this paper uses the YOLOV5 algorithm to identify the target and obtain the initial coordinates. In the early stage, the Labelling software was used to label the targets so as to obtain a model training sample library. Since the environment has interference on target identification, especially when monitoring bridges, the surrounding white clouds may be misidentified. Therefore, the

targets used are not pure white-background targets. Based on the sample library and labels, the YOLOV5 algorithm was used for model training. As it is a one-class model training and the characteristic information of the targets is rather special, the accuracy rate of the model training reaches 99%, as shown in Figure 2(a). The calculation method for the coordinates of the center point of the BOX is $x_0 = (x_1 + x_2)/2$, $y_0 = (y_1 + y_2)/2$. Thus, the coordinates of the center point of the target are obtained. As shown in Figure 2(b), it can be seen from Figure 2(b) that the center of the target can be roughly identified by YOLOV5. However, there is still a certain error compared with the actual center of the target. The error is 5.2 pixels, which is also the intersection recognition problem that needs to be solved in the paper.



(a) Training of the target recognition model



(b) Recognition of the central coordinates of the target

Figure 2: Target training results and identification.

2.3 YOLOV5-MLR Improved Algorithm

As shown in Figure 2(b), due to the complexity of the target image, which is not just in black and white, this type of target can avoid the misidentification of the target caused by the surrounding environment. Since there are many other interfering backgrounds on the target itself, multiple corner points will be detected simultaneously when using the corner detection algorithm, and the center of the target cannot be

accurately located. Therefore, the research in the paper first employs the YOLOV5 algorithm to conduct a rough identification of the center of the target. Obtain the initial values of x_0 , y_0 and z_0 for the target center. Among them, x_0 represents the initial abscissa, y_0 represents the initial ordinate, and z_0 represents the gray value. After obtaining the initial coordinates, the extraction of the target center can be carried out. The main process is as follows:

- (1) Acquisition of the minimum grayscale value within the region. Based on the initial coordinates obtained by the YOLOV5 algorithm, since the inner circle radius of the target is 9 mm, in order to avoid retrieving the pixels on the circle, during the retrieval process, the pixels within the adjacent 5 mm range are retrieved. The number of pixels is represented by q , and the specific formula is as follows.

$$q = d * f / D * a \quad (2)$$

Among them, D represents the distance from the camera to the target, a stands for the size of a pixel, and f represents the focal length. d refers to the retrieval radius, and its value is 5 mm.

The value of q can be calculated through Formula (2). The magnitude of q is determined by the distance D and the focal length f . In addition, on the basis of the initial coordinates of the target, the target searches for the minimum gray value within q adjacent pixels. Usually, this minimum value is mainly distributed on the two intersection lines of the target.

- (2) Acquisition of the coordinates of the pixels that meet the requirements, including the values, where represents the horizontal and vertical coordinates of the pixel in the image, and the value represents the grayscale value of the pixel. According to the grayscale information of the initial coordinates, extract all the points within q pixels around the point and with a value less than $\min(z_0) + 30$, as shown in the following formula.

$$\begin{aligned} x_0 - q < x < x_0 + q \\ y_0 - q < y < y_0 + q \\ z \leq \min(z_0) + 30 \end{aligned} \quad (3)$$

The research in the thesis processes the images through Python programs to obtain all the pixels that meet the conditions and whose values are less than 70. The search results are shown in the following figure.

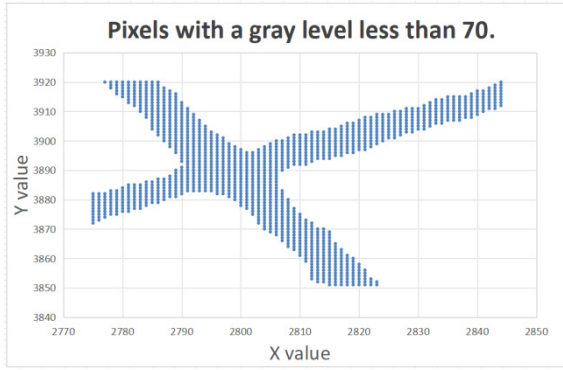


Figure 3: Points with gray values less than 70 within the area.

- (3) Acquisition of the initial intersection line equation: No matter at what angle the cross intersection line at the center of the target is located, the equations of the two intersecting straight lines can be extracted.

First, randomly select two points (x_i, y_i) and (x_j, y_j) from the point library that satisfies the condition of being less than $\min(z_0) + 30$. Meanwhile, it is required that the distance between the two points should be greater than $2q$ pixel values, where q is a positive integer. If the distance from the camera to the target decreases or the camera resolution increases, the value of q will increase correspondingly. On the contrary, if the distance from the camera to the target increases or the resolution decreases, the value of q will decrease accordingly. Therefore, this value is adjusted according to the actual visual measurement. This can ensure that the constructed linear equations are distributed as close to the intersection lines of the target as possible. Meanwhile, it can avoid constructing linear equations with adjacent points, which would otherwise increase the amount of calculation. Therefore, setting a threshold for the distance between two points can improve the calculation efficiency of the target linear equations.

$$\begin{aligned} A_i &= (y_j - y_i) / (x_j - x_i) \\ C_i &= y_i - A_i x_i \quad i, j = 1, \dots, n \\ d_k &= |A_i x_k + B_i y_k + C_i| / \sqrt{A_i^2 + B_i^2} \quad k = 1, \dots, n \end{aligned} \quad (4)$$

As shown in Equation (4), in the equation, A_i represents the slope, C_i represents the intercept, $B_i = 1$, and d_k is the distance from any point in the point library where z is less than $\min(z_0) + 30$ to the generated straight line. Meanwhile, it is required that the number of pixels satisfying $d_k < 1$ should be greater than $4q$, where q is a positive integer.

Therefore, two straight line equations of relatively high quality can be obtained through this method.

$$\begin{aligned} A_1 x + B_1 y + C_1 &= 0 \\ A_2 x + B_2 y + C_2 &= 0 \end{aligned} \quad (5)$$

As shown in Equation (5), B_1 and B_2 are constants with a value of 1. A_1 and A_2 are slopes. C_1 and C_2 are intercepts. And the slopes A_1 and A_2 are two values with opposite signs. As shown in Figure 3, since the two intersecting straight lines are perpendicular to each other, the signs of the slopes of the equations of the two straight lines must be different. From this, two straight lines that are basically close to the target straight lines can be obtained.

- (4) Inspection of the equations of the two intersection lines and acquisition of the optimal straight lines. The intersection line equations obtained through step (3) are relatively close to the target intersection line equations. The error of the intersection point pixels obtained through these intersection line equations is within the range of 2 - 5 pixels, but there still exists a certain degree of error. According to the displacement calculation formula, $d = (D * a * s) / f$, Among them, "a" represents the pixel size, "D" stands for the distance from the camera to the target, "s" represents the number of pixels, and "f" represents the focal length. The camera used in the research of the paper has a fixed focal length of 12 mm, and a 2x zoom with a focal length of 24 mm. The pixel size is 2 μm , and the resolution is 48 million pixels. When the distance is 1 m, the precision is 0.08 mm, and when the distance is 10 m, the precision is 0.8 mm. When the error is 5 pixels, the maximum error is 0.4 mm at a distance of 1 m, and the maximum error is 4 mm at a distance of 10 m. Generally, the error requirement for bridge and building monitoring is at the millimeter level. If the error is controlled within 2 pixels, the maximum error is 0.16 mm at a distance of 1 m, and the maximum error is 1.6 mm at a distance of 10 m, which meets the monitoring requirements. When the distance is relatively close, the intersection coordinates obtained from the initial intersection line equation are sufficient to meet the requirements of bridge monitoring. As the distance increases, the error gradually increases. To further improve the precision, inspection and optimal straight line selection are carried out on the basis of step (3).

Through step (3), n pairs of straight line equations that meet the requirements can be obtained.

Therefore, in order to further reduce the error in the calculation of the intersection points of the target, it is necessary to select the two straight lines with the highest precision from the n pairs of intersection line equations. Thus, after obtaining n pairs of straight line equations that meet the requirements, the target straight lines are selected by the substitution method.

$$\begin{aligned} A_i x_i + C_i = y_{i+1} \quad |y_{i+1} - y_i| &\leq 1 \\ x_j + C_j = y_{j+1} \quad |y_{j+1} - y_j| &\leq 1 \end{aligned} \quad (6)$$

Among them, x_i , y_i , x_j and y_j are the points in the point library where z is less than $\min(z_0) + 30$. In the inspection process, $4q$ points that meet the condition of equation (6) are required, where q is a positive integer. Two target straight lines are determined by this method.

- (5) Target center calculation. Conduct intersection calculation based on A_i , C_i , A_j and C_j obtained in step (4). This intersection is the target center. Here, $B_{i+1}=1$ and $B_j=1$. The coordinates of the target center are shown in the following formula:

$$\begin{aligned} x_{\text{final}} &= (B_j C_i - B_i C_j) / (A_i B_j - A_j B_i) \\ y_{\text{final}} &= (A_i C_j - A_j C_i) / (A_i B_j - A_j B_i) \end{aligned} \quad (7)$$

3 COMPARATIVE ANALYSIS on the APPLICATION of the IMPROVED YOLOV5-MLR ALGORITHM

3.1 Error Analysis of the Improved YOLOV5-MLR Algorithm

In terms of error analysis, the research in the thesis conducts error analysis from two aspects. For the first aspect, a comparative analysis is carried out longitudinally for a single target. During the analysis process, three targets at different distances from the camera are selected, as shown in Figure 4.



Figure 4: YOLOV5 Target center coordinates acquisition.

The equations of n pairs of intersection lines can be obtained through certain steps. The following are the slope and intercept values of any pair of equations among the three targets. Firstly, use YOLOV5 to obtain the coordinates of the targets. Secondly, use the equations of the intersection lines to obtain the initial coordinates of the intersection points. Respectively for $A_{11} = 1.06, C_{11} = 21915$, $A_{12} = -1, C_{12} = 6407.0$, $A_{21} = 1, C_{21} = 1030$, $A_{22} = -1.14, C_{22} = 6652.14$, $A_{31} = -0.94, C_{31} = 7228, A_{32} = 1.1, C_{32} = 753$.

Finally, substitute the known coordinates for checking and determine the optimal intersection line equation and coordinates. Its slope and intercept are $A_{41} = 1.085714, C_{41} = 1861.342857, A_{42} = -1.028571, C_{42} = 6470.714285, A_{51} = -1.088235, C_{51} = 6509.411764, A_{52} = 0.939394, C_{52} = 1189.939394, A_{61} = -0.787234, C_{61} = 6750.148936, A_{62} = 1.11764705, C_{62} = 698$ respectively.

The coordinates of YOLOV5, the initial coordinates, the optimal coordinates and the real coordinates are shown in Table 1.

Table 1: Individual target coordinates at different stages.

Poin t num ber	Coordi nates	YOL OV5	Initial value	Optimal value	Tru e val ue.
1	x	2206	2180.58 2524	2180.10 8844	218 0
	y	4230	4226.41 7476	4228.31 7551	422 8
2	x	2620	2627.16 8224	2623.49 4007	262 3
	y	3660	3657.16 8224	3654.43 3764	365 4
3	x	3194	3174.01 9608	3177.17 9455	317 7
	y	4252	4244.42 1569	4248.96 5245	424 9

For the three targets, through longitudinal analysis of each individual target, it was found that during the process of obtaining the central coordinates of the three targets, the errors of the iterative coordinates were all the smallest, and the errors of the optimal coordinates tended to be around 0. The error results are shown in Figure 5.

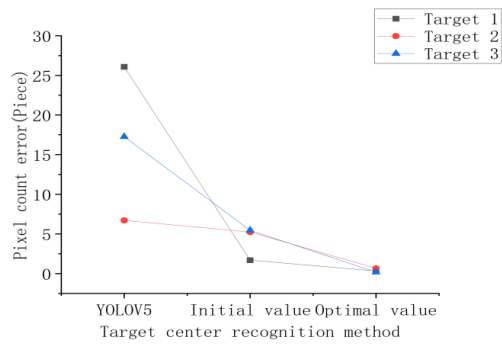


Figure 5: Error statistics plots for the different methods.

In addition to the longitudinal comparison, the thesis research also conducts a lateral comparison based on the actual distances. As shown in the Figure 6 below, it presents the distances between two targets calculated by different methods. Among them, the distance between the camera and the target is 1,469 mm. Through analysis, it was found that the deviations between the distances between the two targets obtained by YOLOV5 and the true values were relatively large. And the initial values of the distances between the two targets obtained through the intersection line equation were relatively close to the true values, but there were still errors and the results were unstable, which was caused by randomness. However, the distances between the two targets calculated according to the optimal linear equation were close to the true values, with errors within 1 mm. Through practical analysis, it was discovered that using the improved YOLOV5-MLR algorithm for target displacement monitoring has a relatively good effect, with high precision and low errors.

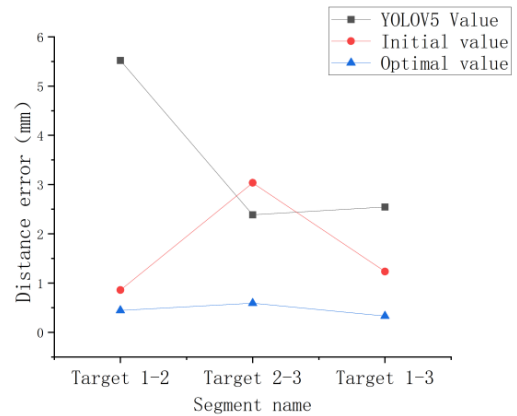
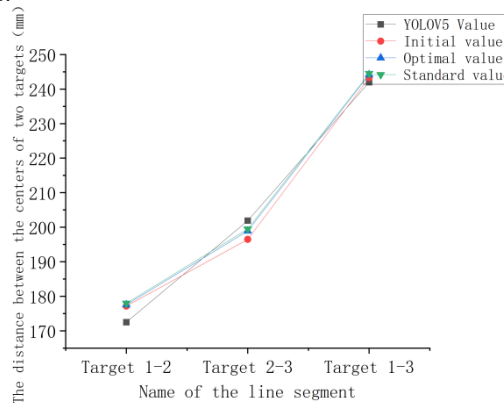


Figure 6: Statistical map of the actual distance between the two targets.

3.2 Application of the YOLOV5-MLR Improved Algorithm in Target Displacement Monitoring

This paper conducts a practical demonstration of bridge displacement monitoring with the on-campus bridge training base as the application scenario. The selected bridge is the Kunpeng Bridge on campus, which is a rather distinctive bridge and a training bridge integrating monitoring and detection. Therefore, applying the target-based visual displacement monitoring technology to this bridge has relatively high teaching value. In this practical application, the target is attached to the bridge pier for monitoring the lateral and longitudinal displacements of the pier. Since the camera cannot achieve high-power zoom and to ensure a relatively high actual resolution of the target, the monitoring distance of this bridge is 2666 mm, the camera focal length is 24 mm, the pixel size is [not provided in the original text], and the accuracy is 0.22 mm. As shown in the following Figure 7, the pixel coordinates of the target measured by the YOLOV5 - MLR improved algorithm are (2130.1, 5968.4), and the actual coordinates in the image plane coordinate system are (473.22, 1325.89) with the unit of mm.



Figure 7: Pixel coordinates and image plane coordinates.

4 CONCLUSION

Bridge safety is a social focus and hot topic. Therefore, bridges should be regularly monitored and early-warning systems should be in place to ensure their normal operation. Existing monitoring methods mainly rely on coordinate measurement using measuring equipment. However, the research in this paper conducts bridge displacement monitoring through computer vision. Through research, it has been found that the improved YOLOV5-MLR algorithm has the following advantages:

- (1) In terms of target selection, targets with relatively complex textures are chosen. The main advantage of complex-textured targets lies in the fact that they can be well distinguished from the surrounding environment. Especially when there are background images such as clouds in the detection environment, traditional black-and-white targets are prone to recognition errors during the identification process. Therefore, choosing relatively complex targets helps to improve the accuracy of target detection.
- (2) Compared with previous corner detection

algorithms, the improved YOLOV5-MLR algorithm takes advantage of the YOLOV5 algorithm. YOLOV5 can quickly and preliminarily locate the center of the target, and has a higher detection efficiency. Moreover, as the target texture becomes complex while ensuring recognition accuracy, there are many corner points in complex-textured targets. As a result, using corner detection algorithms will return multiple results, and the detection results are not unique. However, the improved YOLOV5-MLR algorithm can identify the center of the target with a unique result, which is more helpful for quickly extracting the center point of the target.

- (3) In terms of the recognition accuracy of the target center, it is more precise than both the YOLOV5 and corner detection algorithms. Especially when the target image is affected by factors such as illumination and distance, the results obtained by corner detection are not the center of the target, with an error of several pixels. When the improved YOLOV5-MLR algorithm is used for target center detection, the error can be controlled within the size of one pixel. Its accuracy is more conducive to bridge displacement monitoring and meets the requirements of displacement monitoring specifications. In addition, to improve the adaptability of target center detection, in the future, high-resolution zoom cameras can be used for long-distance target center detection, so as to achieve long-distance bridge displacement monitoring.

ACKNOWLEDGMENTS

This work had been supported by Basic Research Project of Guizhou Provincial Department of Science and Technology, China (Grant No. ZK [2021]-290); Science and Technology Plan Project of Guiyang City, China (Grant No. [2024]-1-7); Soft Science Research Project of Qingzhen City, China (Grant No. [2023]04); Science and Technology Project of Guizhou Provincial Department of Transport, China (Grant No. 2023-123-036); Guizhou Province Science and Technology Plan Project, China (Grant No. GZSTCPT-CXTD[2021]008); Funding for scientific research of Guizhou Communications Polytechnic University (Grant No. KYQD2022006); Key Laboratory of High Performance Restoration Materials for Higher Education Construction Projects in Guizhou Province, China (Grant No. [2023]030).

REFERENCES

- Liu, L., Luo, S., 2024. Data processing in the application of bridge deflection deformation [J]. *Science and Technology Innovation*, (08): 91-94.
- Liao, X., He, Q., Luo, Q., 2024. Application of measuring robot in bridge static load test [J]. *Fujian Building Materials*, (02): 30-32.
- Shan, J., Qi, L., 2024. Bridge structural displacement reconstruction method based on the adaptive Kalman filter GNSS-RTK fused with acceleration data [J]. *Journal of Test Technology*, 38(03): 221-229.
- Liu, Y., Li, Y., 2024. Adaptive FAST corner point detection optimization algorithm based on gray scale mean [J]. *Electro-optic and Control*, 31(02): 65-71+91.
- Shang, M., Wang, K., 2024. Image registration algorithm based on multiscale Harris angular point detection[J]. *Electro-optic and control*, 31(01): 28-32.
- Bao, J., Sun, D., Huang, J., et al., 2024. FAST detection algorithm based on adaptive threshold [J/OL]. *Journal of Shanghai Jiao Tong University*, 1-25 [2024-07-30]. <https://doi.org/10.16183/j.cnki.jsjtu.2023.276>.
- Busca, G., Cigada, A., Mazzoleni, P., et al., 2014. Vibration Monitoring of Multiple Bridge Points by Means of a Unique Vision-Based Measuring System [J]. *Experimental Mechanics*, 54(2):255-271.
- Shang, S., Cao, J., Wang, M., et al., 2024. Research on corner detection algorithms in machine vision [J]. *Computer Measurement and Control*, 32(1): 217-225.
- Xiang, Y., 2010. *Research on image registration technology based on point features*[D]. Shengyang: Northeastern University.
- Lin, P., Li, L., Li, C., 2010. An improved fast SUSAN corner detection algorithm[J]. *Computer and Modernization*, 1(2): 66-68.
- Ding, Y., Wang, J., Qiu, Y., et al., 2013. FAST feature point extraction algorithm based on adaptive threshold[J]. *Command and Control&Simulation*, 35(2): 47-53.
- Lee, J.J., Ho, H.N., Lee, J.H., 2012. A Vision-Based Dynamic Rotational Angle Measurement System for Large Civil Structures [J]. *Sensors, Molecular Diversity Preservation International*, 12(6): 7326-7336.
- Hu, J., Zhu, Q., Zhang, Q., 2022. Global Vibration Comfort Evaluation of Footbridges Based on Computer Vision[J]. *Sensors*, 22(18): 7077.
- Zhou, X., Wang, X., Liu, Y., et al., 2023. Method of vertical displacement measurement based on the YOLOv5 target detection model and vision [J]. *Geospatial Information*, 21(12): 25-28.